Received: 26 September 2022 | Accepted: 16 March 2023

DOI: 10.1002/jmv.28686

RESEARCH ARTICLE

JOURNAL OF MEDICAL VIROLOGY WILEY

Omicron-induced interferon signaling prevents influenza A H1N1 and H5N1 virus infection

Denisa Bojkova[1] | Marco Bechtel[1] | Tamara Rothenburger[1] | Joshua D. Kandler[1] | Lauren Hayes[2] | Ruth Olmer[3] | Ulrich Martin[3] | Danny Jonigk[4,5] | Sandra Ciesek[1,6,7] | Mark N. Wass[2] | Martin Michaelis[2] | Jindrich Cinatl jr.[1,8]

[1]Institute for Medical Virology, University Hospital, Goethe University, Frankfurt am Main, Germany

[2]School of Biosciences, University of Kent, Canterbury, UK

[3]Leibniz Research Laboratories for Biotechnology and Artificial Organs (LEBAO), Department of Cardiothoracic, Transplantation and Vascular Surgery (HTTG), REBIRTH-Research Center for Translational Regenerative Medicine, Biomedical Research in Endstage and Obstructive Lung Disease Hannover (BREATH), German Center for Lung Research (DZL), Hannover Medical School, Hannover, Germany

[4]Institute of Pathology, Hannover Medical School (MHH), Hannover, Germany

[5]Biomedical Research in Endstage and Obstructive Lung Disease Hannover (BREATH), The German Center for Lung Research (Deutsches Zentrum für Lungenforschung, DZL), Hannover Medical School (MHH), Hannover, Germany

[6]German Center for Infection Research, DZIF, External partner site, Frankfurt am Main, Germany

[7]Fraunhofer Institute for Molecular Biology and Applied Ecology (IME), Branch Translational Medicine und Pharmacology, Frankfurt am Main, Germany

[8]Dr. Petra Joh-Forschungshaus, Frankfurt am Main, Germany

Correspondence
Jindrich Cinatl jr., Institute for Medical Virology, University Hospital, Goethe University, Paul Ehrlich-Straße 40, 60596 Frankfurt am Main, Germany.
Email: Cinatl@em.uni-frankfurt.de

Martin Michaelis, School of Biosciences, University of Kent, Canterbury CT2 7NJ, UK.
Email: M.Michaelis@kent.ac.uk

Funding information
Goethe-Corona-Fonds; Frankfurter Stiftung für krebskranke Kinder; Bundesministerium für Bildung und Forschung

Abstract

Recent findings in permanent cell lines suggested that SARS-CoV-2 Omicron BA.1 induces a stronger interferon response than Delta. Here, we show that BA.1 and BA.5 but not Delta induce an antiviral state in air-liquid interface cultures of primary human bronchial epithelial cells and primary human monocytes. Both Omicron subvariants caused the production of biologically active types I (α/β) and III (λ) interferons and protected cells from super-infection with influenza A viruses. Notably, abortive Omicron infection of monocytes was sufficient to protect monocytes from influenza A virus infection. Interestingly, while influenza-like illnesses surged during the Delta wave in England, their spread rapidly declined upon the emergence of Omicron. Mechanistically, Omicron-induced interferon signaling was mediated via double-stranded RNA recognition by MDA5, as MDA5 knockout prevented it. The JAK/STAT inhibitor baricitinib inhibited the Omicron-mediated antiviral response, suggesting it is caused by MDA5-mediated interferon production, which activates interferon receptors that then trigger JAK/STAT signaling. In conclusion, our study (1) demonstrates that only Omicron but not Delta induces a substantial interferon response in physiologically relevant models, (2) shows that

Omicron infection protects cells from influenza A virus super-infection, and (3) indicates that BA.1 and BA.5 induce comparable antiviral states.

KEYWORDS
antiviral state, BA.1, BA.5, COVID-19, Delta, influenza, interferon, monocytes, SARS-CoV-2, super-infection

1 | INTRODUCTION

SARS-CoV-2, the coronavirus that causes COVID-19, has caused the worst pandemic since the Spanish Flu in 1918–1920.[1] Virus-induced interferon signaling has been shown to be critically involved in determining COVID-19 severity.[1] Individuals with defects in their interferon response are predisposed to life-threatening COVID-19,[1] and a particularly pronounced interferon-related innate immune response is anticipated to contribute to the lower COVID-19 severity observed in children.[2]

Recent findings suggested that SARS-CoV-2 Omicron BA.1 displays a lower interferon antagonism than Delta.[3,4] BA.1 and Delta viruses showed a similar replication pattern in interferon-deficient Vero cells, but BA.1 replication was attenuated relative to Delta in interferon competent Calu-3, Caco-2, and Caco-2-F03 (a highly SARS-CoV-2-susceptible Caco-2 subline[5]) cells.[3,6,7] Moreover, BA.1 induced a more pronounced interferon response than Delta.[3,4]

To study the interferone response by different SARS-CoV-2 variants in physiologically more relevant models than the previously used cell lines, we here investigated Delta, BA.1, and BA.5 replication in air-liquid interface (ALI) cultures of primary human bronchial epithelial (HBE) cells and primary human monocytes. Moreover, previous studies had focused on interferon signaling and production as read-outs, which indicate an interferon response but do not demonstrate whether SARS-CoV-2 variants actually induce a biologically relevant antiviral state. Thus, we here determined the impact of Delta, BA.1, and BA.5 infection on influenza A virus replication in ALI HBE cultures (H1N1) and monocytes (H1N1, H5N1). Interferon signaling is considered to be a major influenza A virus restriction factor.[8] Thus, investigating the impact of SARS-CoV-2 on influenza A virus infection enables a conclusion on whether SARS-CoV-2-induced interferon signaling translates into an antiviral state that inhibits virus replication.

2 | METHODS

2.1 | Cell lines

ARPE cells (DSMZ) were cultured in was grown at 37°C in minimal essential medium (MEM) supplemented with 10% foetal bovine serum (FBS), 100 IU/mL of penicillin, and 100 µg/mL of streptomycin. All culture reagents were purchased from Sigma-Aldrich.

HEK293 (HEK-Blue™ reporter cells, InvivoGen) -IFN-α/β and -IFN-λ cells were cultivated in Dulbecco's modified Eagle medium (DMEM) (Gibco, ThermoFisher Scientific) with 10% heat-inactivated FBS (Sigma), Pen-Strep (100 U/mL-100 µg/mL) (Sigma), 100 µg/mL Normocin™ (InvivoGen), and selection antibiotics (interferon-α/β: blasticidin, zeocin; IFN-λ: blasticidin, puromycin, zeocin) at 37°C and 5% CO_2.

A549-ACE2/TMPRSS2 and ACE2/TMPRSS2 MDA5 KO cells (Invivogen) were grown in DMEM supplemented with 2 mM L-glutamine, 4.5 g/L glucose, 10% (vol/vol) heat-inactivated FBS (30 min at 56°C), PenStrep (100 U/mL–100 µg/mL), 100 µg/mL normocin, 10 µg/mL blasticidin, 10 µg/mL blasticidin, 100 µg/mL hygromycin, 0.5 µg/mL puromycin, and 100 µg/mL of zeocin.

All cell lines were regularly tested for mycoplasma contamination.

2.2 | ALI cultures

Primary bronchial epithelial cells were isolated from lung explant tissue of emphysema patients as previously described.[9] Tissue use was approved by the ethics committee of the Hannover Medical School (MHH, Hannover, Germany, number 2701–2015) in compliance with The Code of Ethics of the World Medical Association and subject to written informed consent.

Basal cells were expanded in Keratinocyte-SFM medium supplemented with bovine pituitary extract (25 µg/mL), human recombinant epidermal growth factor (0.2 ng/mL, all from Gibco), isoproterenol (1 nM; Sigma), Antibiotic/Antimycotic Solution (Sigma-Aldrich), and MycoZap Plus PR (Lonza, Cologne) and cryopreserved until further use.

Cells were resuscitated, passaged once in PneumaCult-Ex Medium (StemCell Technologies), and seeded on transwell inserts (12-well plate, Sarstedt) at 4×10^4 cells/insert. Once the cell layers reached confluency, the medium on the apical side of the transwell was removed, and medium in the basal chamber was replaced with PneumaCult ALI Maintenance Medium (StemCell Technologies), including Antibiotic/Antimycotic Solution (Sigma-Aldrich) and MycoZap Plus PR (Lonza). Medium was changed and cell layers were washed with phosphate-buffered saline (PBS) every other day.

Criteria for successful differentiation were the development of ciliated cells, ciliary movement, an increase in transepithelial electric resistance (indicating tight junction formation), and mucus production.

2.3 | SARS-CoV-2 variants preparation

SARS-CoV-2 Omicron BA.1 (B.1.1.529: FFM-SIM0550/2021, EPI_ISL_6959871, GenBank ID OL800702), Delta (B.1.167.2: FFM-IND8424/2021, GenBank ID MZ315141), and Omicron BA.5 (GenBank ID OP062267) were isolated in Caco-2-F03 cells as previously described[5,10] and stored at −80°C. Virus titres were determined as TCID50/mL.

2.4 | Influenza A virus strains H1N1 and H5N1

The H1N1 influenza strain A/New Caledonia/20/99 (World Health Organization [WHO] Influenza Center [National Institute for Medical Research, London, UK]) and A(H1N1)pdm09 strain A/HH/01/2009 (obtained from M. Eickmann, Institute of Virology, Marburg, Germany) were propagated in MDCK cells (ATCC, CCL-34) in medium containing 2 µg/mL trypsin. Virus stocks were stored at −80°C. The H5N1 influenza strain A/Vietnam/1203/04 (WHO Influenza Center [National Institute for Medical Research, London, UK]). H5N1 virus stocks were prepared by infecting Vero cells, and aliquots were stored at −80°C. Virus titres were determined as TCID50/mL.

2.5 | Barrier integrity measurement

For transepithelial electrical resistance (TEER) measurement, medium was added to the apical side 30 min before measurement with a chopstick electrode connected to a Volt-Ohm-meter (Millicell® ERS-2, Merck) according to the manufacturer's instructions. Blank inserts served as baseline.

2.6 | Activation of caspase 3/7

Caspase 3/7 activity was measured using the Caspase-Glo assay kit (Promega), according to the manufacturer's instructions as previously described.[5]

2.7 | Super-infection assay in ALI HBE

ALI HBE cultures were infected with SARS-CoV-2 (MOI 1) from the apical site for 2 h. Then the infection medium was removed and cells were washed three times with PBS. H1N1 A/New Caledonia/20/99 (MOI 2) was added 48 h post-SARS-CoV-2 infection for 2 h. Then the infection medium was removed and cells were washed three times with PBS.

2.8 | Detection of extracellular and intracellular RNA

SARS-CoV-2 RNA from the apical washes of the ALI HBE culture was isolated using QIAamp Viral RNA Kit (Qiagen) according to the manufacturer's instructions. RNA was subjected to OneStep qRT-PCR analysis using the Luna Universal One-Step RT-qPCR Kit (New England Biolabs) and a CFX96 Real-Time System, C1000 Touch Thermal Cycler (Bio-Rad). Primers were adapted from the WHO protocol29 targeting the open reading frame for RNA-dependent RNA polymerase (RdRp): RdRP_SARSr-F2 (GTGARATGGT-CATGTGTGGCGG) and RdRP_SARSr-R1 (CARATGTTAAASACAC-TATTAGCATA) using 0.4 µM per reaction. Standard curves were created using plasmid DNA (pEX-A128-RdRP) as previously described.[11]

Intracellular RNA isolation was carried out using the RNeasy 96 QIAcube HT Kit (Qiagen) according to the manufacturer's protocol. Detection of selected targets was performed with Luna® Universal One-Step RT-qPCR (New England BioLabs Inc.) according to the manufacturer's protocol using the following primers: TBP (fw: 5′-ATCAGAACAACAGCCTGCC-3′; rev: 5′-GGTCAGTCCAGTGCCAT AAG-3′); SARS-CoV-2 E gene (fw: 5′-ACAGGTACGTTAATAGTTA ATAGCGT-3′; rev: 5′-ATATTGCAGCAGTACGCACACA-3′); ISG15 (fw: 5′-GAGAGGCAGCGAACTCATCT-3′; rev: 5′-AGGGACACCTG GAATTCGTT-3′); MX1 (fw: 5-TTTTCAAGAAGGAGGCCAGCAA-3′; rev: 5′-TCAGGAACTTCCGCTTGTCG-3′); H5N1 H5 gene (fw: 5′-GCCATTCCACAACATACACCC-3′; rev: 5′-CTCCCCTGCTCATTGC TATG-3′); H5N1 M gene (fw: 5′-TTCTAACCGAGGTCGAAACG-3′; rev: 5′-ACAAAGCGTCTACGCTGCAG-3′); IAV NP-messenger RNA (mRNA) (fw: 5′-GACTCACATGATGATCTGGCA-3′; rev: 5′-CTTGT TCTCCGTCCATTCTCA-3′); IAV NP-gRNA (fw: 5′-AACGGCTGGT CTGACTCACATGAT-3′; rev: 5′-AGTGAGCACATCCTGGGATCC ATT-3′).

2.9 | Immunoblot analysis

Whole-cell lysates were prepared using Triton-X sample buffer containing protease inhibitor cocktail (Roche). Protein concentrations were assessed using DC Protein assay reagent (Bio-Rad Laboratories). Proteins were separated by sodium dodecyl sulfate-polyacrylamide gel electrophoresis and transferred to nitrocellulose membranes (Thermo Scientific). For protein detection the following primary antibodies were used: GAPDH (#2118, 1:4000, Cell Signaling), γH2AX (#9718, 1:1000, Cell Signaling), H1N1 (Influenza A Virus) Nucleoprotein (#bs-4976R, 1:4000, Bioss), ISG15 (#sc-166755, 1:200, Santa Cruz Biotechnology), MDA5 (#5321, 1:1000, Cell Signaling), Mx1 (#37849, 1:1000, Cell Signaling), OAS1 (#14498, 1:1000, Cell Signaling), PARP (#9542, 1:1000, Cell Signaling), PKR (#12297, 1:1000, Cell Signaling), SARS-CoV-2 Nucleocapsid (#40143-R019, 1:10 000, Sino Biological), STAT1 (#9172, 1:1000, Cell Signaling), phospho-STAT1 Y701 (#9171, 1:1000, Cell Signaling), TBK1 (#3013, 1:1000, Cell Signaling), phospho-TBK1 S172 (#5483,

1:1000, Cell Signaling), USP18 (#4813, 1:2000, Cell Signaling) and RIG1 (#3743, 1:1000, Cell Signaling). Protein bands were visualized using IRDye-labeled secondary antibodies at dilution 1:40 000 (LI-COR Biotechnology, IRDye®800CW Goat anti-Rabbit, #926-32211 and IRDye®800CW Goat anti-Mouse IgG, #926-32210) and Odyssey Infrared Imaging System (LI-COR Biosciences).

2.10 | Interferon detection

Types I and III interferons were detected using HEK-Blue™ IFN-α/β (type I) and HEK-Blue™ IFN-λ (type III) cells according to the manufacturer's protocol. Cells were washed twice with PBS, detached tapping the flask, centrifuged at 200*g* for 5 min, and resuspended in Test Medium (DMEM, 4.5 g/L glucose, 2 mM L-glutamine, 10% (vol/vol) heat-inactivated FBS, 50 U/mL penicillin, 50 µg/mL streptomycin, 100 µg/mL Normocin™) at 280 000 cells/mL. A total of 20 µL cell culture supernatant and 180 µL cell suspension were added to the wells of 96-well plates and incubated at 37°C and 5% CO_2 for 24 h. After incubation, 20 µL supernatant was removed and incubated with 180 µL QUANTI-Blue™ Solution for 1–3 h. Secreted embryonic alkaline phosphatase levels were determined using a spectrophotometer at 620 nm.

2.11 | Influenza A virus entry assay

The influenza A virus entry assay was performed as previously described.[12] ALI HBE cultures were infected with Omicron BA.1 (MOI 1) from the apical site for 2 h. Then, the infection medium was removed and the cells were washed three times with PBS. H1N1 A/New Caledonia/20/99 (MOI 1) was added apically 48 h post-SARS-CoV-2 infection. After a 1-h incubation period at 4°C, the infection medium was removed and the cells were washed three times with either PBS (4°C) or with PBS/HCl (pH 1.3, 4°C) followed by two washing steps with PBS before an additional 1-h incubation period at 37°C, after which genomic influenza A virus RNA was harvested for analysis.

2.12 | Human peripheral blood mononuclear cell (PBMC) isolation

Human PBMCs were isolated from buffy coats of healthy donors (RK-Blutspendedienst Baden-Württemberg-Hessen, Institut für Transfusionsmedizin und Immunhämatologie Frankfurt am Main, Germany). After centrifugation on a Ficoll (Pancoll, PAN-Biotech) density gradient, mononuclear cells were collected from the interface, washed with PBS, and plated on cell culture dishes (Cell+, Saarstedt) in RPMI1640 (Gibco, ThermoFisher Scientific) supplemented with 100 IU/mL penicillin and 100 g/mL streptomycin. After incubation for 90 min (37°C, 5% CO_2), nonadherent cells were removed, and the medium was changed to RPMI1640 supplemented with 100 IU/mL penicillin, 100 µg/mL of streptomycin, and 3% human serum (RK-Blutspendedienst Baden-Württemberg-Hessen, Institut für Transfusionsmedizin und Immunhämatologie Frankfurt am Main, Germany).

2.13 | Super-infection assay in human PBMCs

Human PBMCs were infected with SARS-CoV-2 variants (MOI 1) for 2 h in infection medium (RPMI1640 supplemented with 100 IU/mL penicillin and 100 g/mL streptomycin, 1% heat-inactivated FBS) at 37°C/5% CO_2. Then, cells were washed twice with PBS and incubated for 24 h in infection medium, before infection with H1N1/New Caledonia/20/99 (MOI 2) or H5N1 A/Vietnam/1203/04 (MOI 1) for 2 h. Mock-infected cells served as controls.

2.14 | Immunofluorescence labeling of influenza A

Cells were fixed with methanol/aceton (60/40) and blocked with 2% BSA and 5% goat serum. Staining was performed using anti-Influenza A Antibody, nucleoprotein (1:1500 dilution, #MAB8251 Merck KGaA) and secondary Alexa Fluor™ 647 antibody (1:1000 dilution, #A-21246 ThermoFisher Scientific) and DAPI (0.2 µg/mL). Cells were imaged and analysed using Tecan Spark® Cyto.

2.15 | Preparation and antiviral testing of conditioned ALI HBE culture medium

Omicron BA.1-infected or mock-treated ALI HBE cultures were incubated with 500 µL of cell culture medium at the apical site 48 h postinfection. After 30 min, the medium was collected, UV-inactivated for 5 min, aliquoted, and stored at −80°C. For the determination of antiviral activity, confluent ARPE cell cultures in 96-well plates were treated with conditioned media at increasing dilutions for 24 h. Subsequently, cells were infected with H1N1 A/New Caledonia/20/99 (MOI 1) for another 24 h. Infected cells were detected by immunofluorescent staining for influenza A virus NP.

2.16 | Blocking of types I and III IFN signaling

ARPE cells were pretreated for 1 h with either Recombinant Viral B18R Protein (type I IFN signaling, 100 ng/mL, #8185-BR R&D Systems, Inc.), Anti-Human IFN-λ Receptor 1, Clone MMHLR-1 (type III IFN signaling 100 ng/mL, #21885 pbl Assay Science), a mouse IgG1 control, or cell culture medium (mock). Then, conditioned media from mock- or Omicron BA.1-infected ALI HBE cultures were added and incubated for 24 h. After this, ARPE cells were infected with H1N1 A/New Caledonia/20/99 (MOI 1) and incubated for 24 h. Influenza A virus infection was detected by immunostaining for influenza A virus

NP. Betaferon (10^2 IU/mL) or IFNλ3 (1.25 μg/mL) served as positive controls.

Human PBMCs were infected with Omicron BA.1 (MOI 1) or left untreated for 2 h. After infection, cells were either treated with Human Type 1 IFN Neutralizing Antibody Mixture (#39000-1, pbl Assay Science) at 1:50 dilution, Anti-Human IFN-λ Receptor 1, Clone MMHLR-1 (type III IFN signaling 100 ng/mL, #21885 pbl Assay Science), or left untreated. After 24 h, cells were infected with H1N1 A/New Caledonia/20/99 (MOI 1) for 2 h and subsequently again treated with either type I or type III IFN blocking antibody. After a further 24 h, intracellular RNA was harvested for analysis.

2.17 | Statistics

Results are expressed as the mean ± standard deviation (*SD*) of the number of biological replicates indicated in figure legends. Statistical significance is depicted directly in graphs and the statistical tests used for the calculation of *p* values are indicated in the figure legends.

3 | RESULTS

3.1 | Infection kinetics and interferon response induction by Omicron BA.1 and Delta in ALI cultures of primary HBE cells

BA.1 displayed faster replication kinetics than Delta in ALI HBE cultures (Figure 1), as indicated by high SARS-CoV-2 nucleoprotein (NP), genomic RNA levels, and caspase 3/7 activity (which reflects SARS-CoV-2 replication independently of whether the virus causes cytotoxicity resulting in a cytopathogenic effect in a cell culture model[5]) (Figure 1B–D). However, the replication of both SARS-CoV-2 variants resulted in comparable peak NP and genomic RNA levels (Figure 1B–D). While the BA.1 levels declined after a peak (at 24 h postinfection for NP and 72 h for genomic RNA), Delta levels continued to increase until 120 h postinfection (Figure 1B–D). These findings are in accordance with previous findings showing that BA.1 replicates faster than other variants in bronchial cells.[13] Independently of the replication kinetics BA.1 and Delta caused similar reductions of the ALI HBE barrier integrity (Figure 1E).

Also in agreement with previous findings,[3,4,14] BA.1 induced a stronger interferon response than Delta, as indicated by the abundance and phosphorylation levels of a range of proteins involved in interferon signaling (Figure 1F). Moreover, only BA.1 but not Delta induced the secretion of biologically active interferon-α/β (Figure 1G) and -λ (Figure 1H) by ALI HBE cultures, as demonstrated using HEK-reporter cell lines.

Interferon-α/β peaked at 24 h postinfection (Figure 1G), which was followed by a return to basal levels, whereas interferon-λ remained elevated until 120 h postinfection (Figure 1H). Short-term interferon type I (α/β) responses cause a protective antiviral response, while long-term interferon activity is associated with potentially deleterious inflammation.[15] In contrast, sustained interferon type III (λ) responses inhibit respiratory virus replication at epithelial barriers in the respiratory tract and prevent excessive inflammation.[15,16] Hence, the interferon types I and III responses observed in BA.1-infected ALI HBE cultures add further evidence explaining why Omicron is less pathogenic than other SARS-CoV-2 variants like Delta.[17]

3.2 | JAK/STAT inhibition suppresses BA.1-induced interferon signaling and increases BA.1 replication in ALI HBE cell cultures

Interferon signaling can be induced in a STAT1-dependent and -independent manner.[1,18] Inhibition of JAK/STAT signaling using the JAK inhibitor baricitinib significantly increased BA.1 replication in ALI HBE cultures (Figure 2), as indicated by genomic RNA copy numbers (3.9-fold, Figure 2B) and cellular NP levels (1.7-fold, Figure 2C). In contrast, Delta only displayed a nonsignificant trend towards higher genomic RNA copy numbers (2.1-fold, Figure 2B) and cellular NP levels (1.4-fold, Figure 2C) in the presence of baricitinib. Baricitinib did not exert significant effects on BA.1- and Delta-mediated caspase 3/7 activation (Figure 2D) and the ALI HBE barrier function (Figure 2E), although there was a nonsignificant trend towards enhanced caspase 3/7 activity in BA.1-infected ALI HBE cultures (Figure 2D).

Western blot analysis confirmed that baricitinib not only increased BA.1 replication but also suppressed BA.1-induced interferon signaling (Figure 2F). Taken together, these findings indicate that the pronounced interferon response induced by BA.1 is mediated via STAT1 and that it attenuates BA.1 replication.

3.3 | BA.1-induced interferon signaling protects ALI HBE cell cultures from H1N1 influenza A virus super-infection

Next, we here infected ALI HBE cultures with BA.1 or Delta (both MOI 1) for 48 h before infection with H1N1 influenza A virus (A/New Caledonia/20/99, MOI 2) (Figure 3A) to examine whether the BA.1-induced interferon response may induce an antiviral state that interferes with H1N1 replication. Infection controls confirmed that both BA.1 and Delta replication as well as BA.1- and Delta-induced interferon induction were comparable to the data presented in Figure 1 (Figure S1).

Determination of H1N1 nucleoprotein (NP) levels indicated that only BA.1 but not Delta suppressed H1N1 A/New Caledonia/20/99 (Figure 3B,C) and A(H1N1)pdm09 strain A/HH/01/2009 (Figure S2) infection in ALI HBE cultures (Figure 3B,C).

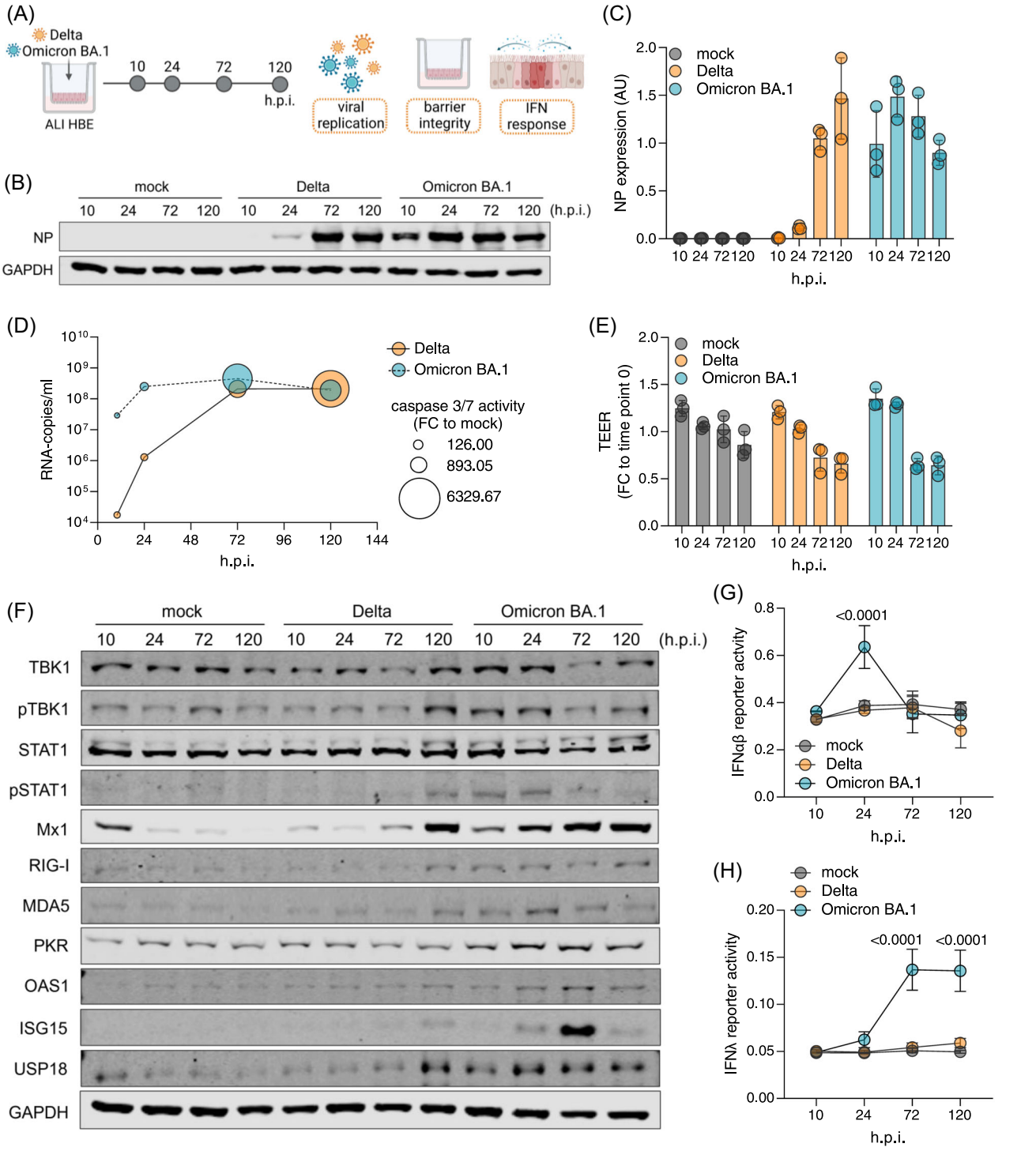

FIGURE 1 Infection kinetics and interferon response induction by Omicron BA.1 and Delta in air-liquid-interface (ALI) cultures of primary human bronchial epithelial (HBE) cells. (A) Schematic depiction of the experimental set-up. (B) Immunoblot of cellular SARS-CoV-2 nucleoprotein (NP) levels in BA.1- and Delta (MOI 1)-infected ALI HBE cultures at different time points postinfection. (C) Quantification of NP levels (mean ± *SD*) by ImageJ. (D) SARS-CoV-2 genomic RNA copy numbers (Y axis) and caspase 3/7 activity (bubble size) determined in the apical medium of BA.1- and Delta (MOI 1)-infected at different time points postinfection. (E) Evaluation of barrier integrity by measurement of TEER in BA.1- and Delta (MOI 1)-infected ALI HBE cultures at different time points postinfection. Bars represents mean ± *SD* of three biological replicates. (F) Immunoblot indicating cellular levels of proteins involved in interferon signaling in BA.1- and Delta (MOI 1)-infected ALI HBE cultures at different time points postinfection. (G, H) Interferon (IFN)-α/β (G) and IFNλ (H) responses induced in HEK reporter cell lines by apical washes from BA.1- and Delta (MOI 1)-infected ALI HBE cultures collected at different time points postinfection. All *p* values were determined by one-way ANOVA with subsequent Tukey's test. ANOVA, analysis of variance

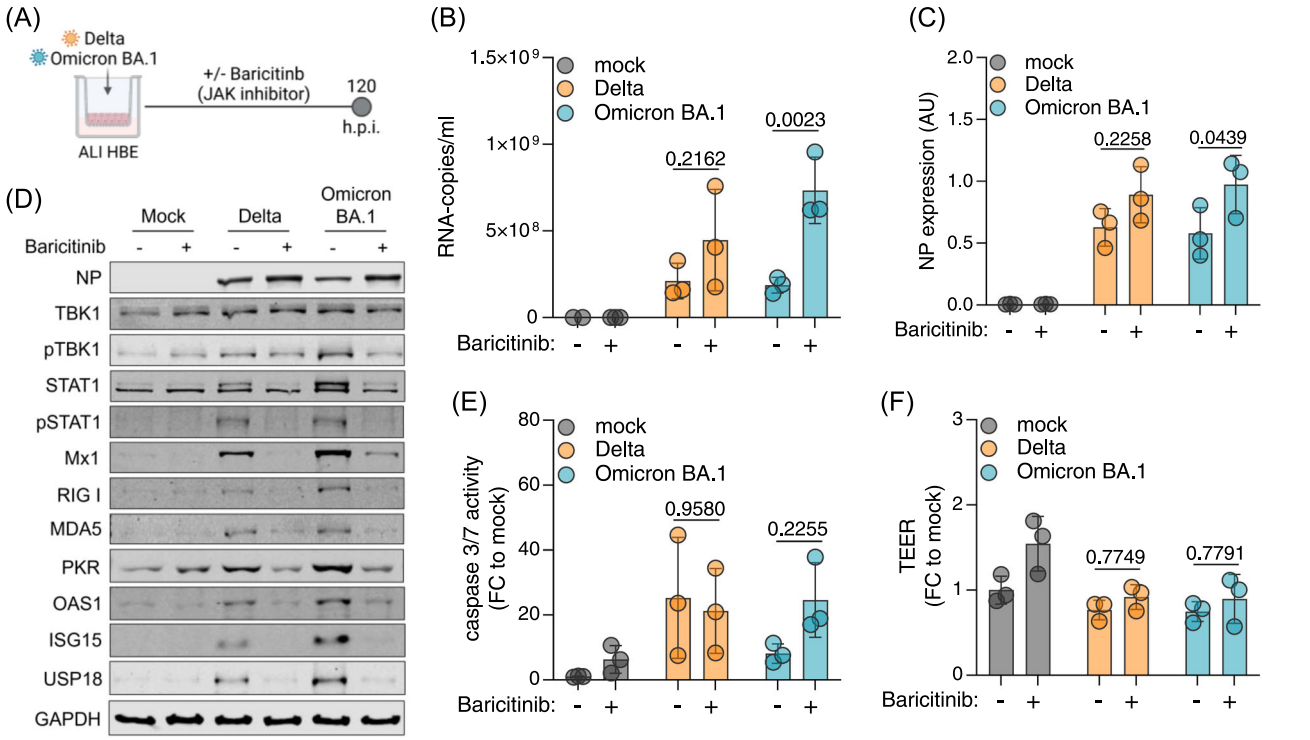

FIGURE 2 Inhibition of JAK/STAT signaling promotes Omicron BA.1 replication. (A) Schematic depiction of the experimental set-up. (B) SARS-CoV-2 genomic RNA copies in apical wash of air-liquid-interface (ALI) human bronchial epithelial (HBE) cultures 120 h post-SARS-CoV-2 (MOI 1) infection in the absence or presence of the JAK inhibitor baricitinib (1 μM). Bars represent mean ± *SD* of three biological replicates. (C) NP levels in SARS-CoV-2 (MOI 1)-infected ALI HBE cultures in the absence or presence of baricitinib (1 μM) as determined by immunoblotting. Bars represent mean ± *SD* of three biological replicates. (D) Caspase 3/7 activation in apical washes of SARS-CoV-2 (MOI 1)-infected ALI HBE cultures in the absence or presence of baricitinib (1 μM) 120 h postinfection. Bars display mean ± *SD* of three biological replicates. (E) Barrier integrity in SARS-CoV-2 (MOI 1)-infected ALI HBE cultures in the absence or presence of baricitinib (1 μM) measured by TEER at 120 h postinfection. Mean ± SD of three biological replicates is presented. (F) Immunoblot indicating cellular levels of proteins involved in interferon signaling in SARS-CoV-2 (MOI 1)-infected ALI HBE cultures at 120 h postinfection in the presence or absence of baricitinib (1 μM). All *p* values were calculated by the Student *t*-test. TEER, transepithelial electrical resistance

H1N1 super-infection did not significantly change SARS-CoV-2 levels in ALI HBE cultures (Figure 3D).

Genomic H1N1 NP RNA and H1N1 NP mRNA levels confirmed that only BA.1 caused a significant reduction of H1N1 replication (Figure 3E). Moreover, only BA.1 infection prevented H1N1-induced cytotoxicity as indicated by TEER measurement (Figure 3F). Influenza A virus replication is associated with the induction of apoptosis and DNA damage induction in host cells,[19,20] and PARP cleavage and γH2AX levels also confirmed that BA.1 infection suppressed H1N1-induced cytotoxicity (Figure 3G,H).

The analysis of proteins involved in interferon signaling showed that also in the presence of H1N1 only BA.1 induced a pronounced interferon response (Figure 3I). In agreement, only BA.1-infected (but not of Delta-infected) ALI HBE cultures produced biologically active types I (α/β) and III (λ) interferons, as demonstrated using HEK-reporter cell lines (Figure 3J,K). Taken together, these findings indicate that only BA.1 but not Delta induces an interferon-mediated antiviral state in ALI-HBE cultures that protects them from H1N1 infection.

3.4 | Inhibition of JAK/STAT signaling promotes H1N1 influenza A virus replication in BA.1-infected cells

Next, we investigated the effect of the JAK inhibitor on the BA.1-mediated suppression of H1N1 replication (Figure 4A). In agreement with the data presented in Figures 2 and 3, baricitinib increased BA.1 replication as indicated by genomic RNA copies of the viral RNA-dependent RNA polymerase gene (Figure 4B). Moreover, baricitinib prevented the BA.1-mediated inhibition of H1N1 replication as indicated by H1N1 NP mRNA (4.0-fold increase) and genomic RNA (61-fold increase) levels (Figure 4C) and H1N1 NP protein (11-fold increase) levels (Figure 4D,E).

In line with our previous findings, baricitinib also antagonized BA.1-induced suppression of H1N1-induced apoptosis as indicated by PARP cleavage and H1N1-induced DNA damage as indicated by cellular γH2AX levels (Figure 4F,G). Furthermore, baricitinib abrogated the BA.1-mediated protection of the ALI HBE barrier integrity from H1N1-induced cytotoxicity (Figure S3). Notably, H1N1

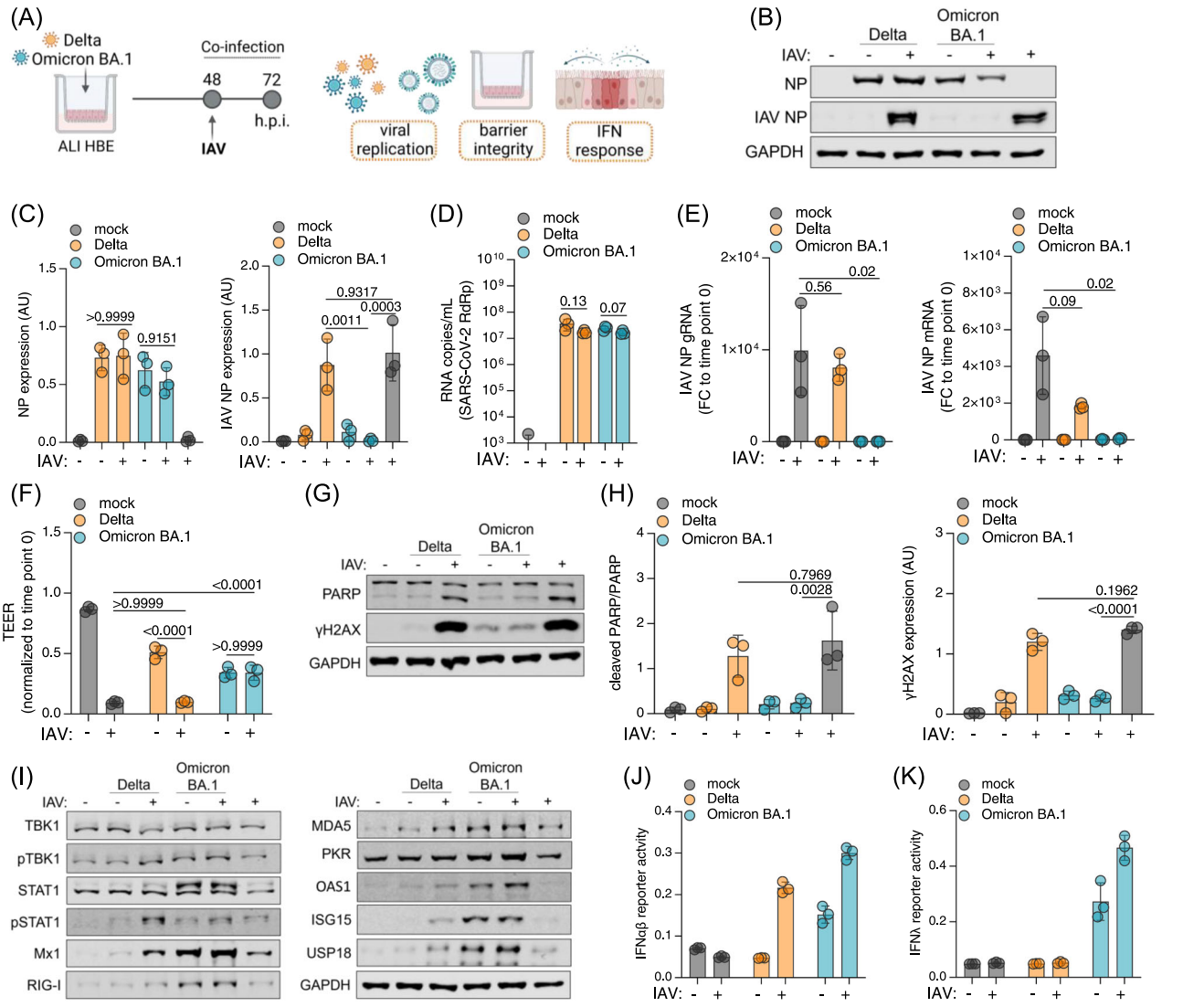

FIGURE 3 Omicron BA.1 but not Delta infection prevents H1N1 influenza A virus (IAV) replication. (A) Schematic of the experimental set-up. (B) Immunoblot of the SARS-CoV-2 nucleoprotein (NP) and H1N1 IAV NP levels 24 h postinfection with H1N1 strain A/New Caledonia/20/99 (MOI 2). (C) Quantification of immunoblots from (B). Bars represent mean ± *SD* of three biological replicates. All *p* values were calculated by two-way ANOVA. (D) Genomic RNA copies of the SARS-CoV-2 RNA-dependent RNA polymerase (RdRp) in the apical wash of ALI HBE cultures 24 h postinfection with H1N1 (MOI 2). Values represent means ± *SD* of three biological replicates. All *p* values were determined by the Student *t*-test. (E) IAV NP genomic RNA (gRNA, left) or mRNA (right) levels 24 h postinfection with H1N1 (MOI 2). Bars display means ± *SD* of three biological replicates. A *p* values were determined by the Student *t*-test. (F) Barrier integrity measure by transepithelial electric resistance (TEER) in single- or coinfected ALI cultures. Bars display means ± *SD* of three biological replicates. All *p* values were calculated by two-way ANOVA. (G) Immunoblot of PARP cleavage and γH2AX after single- or co-infection. (H) Quantification of the immunoblots from (G). Values represent the mean ± *SD* of three biological replicates. All *p* values were calculated by two-way ANOVA. (I) Immunoblots displaying the levels of proteins involved in interferon signaling in single- and coinfected ALI HBE cultures. (J, K) Interferon (IFN)α/β (J) or IFNλ (K) signaling in HEK-reporter cell lines incubated with apical washes of single- and co-infected ALI HBE cultures 24 h postinfection with H1N1 (MOI 2). ALI, air-liquid interface; ANOVA, analysis of variance; HBE, human bronchial epithelial; mRNA, messenger RNA

influenza A virus entry experiments showed that similar amounts of influenza A virus are internalized by BA.1- and mock-infected cells. This indicates that the BA.1-mediated antiviral state is caused by mechanisms that interfere with H1N1 infection post entry (Figure S4).

As indicated by the cellular levels of proteins involved in interferon signaling, the BA.1-induced interferon response was not affected by H1N1 (Figure 4H). Moreover, baricitinib inhibited interferon signaling in response to ALI HBE infection with either single virus and after co-infection with both viruses (Figure 4H) and suppressed interferon-α/β and -λ production (Figure 4I,J).

The pattern recognition receptor MDA5 was previously shown to be critically involved in the SARS-CoV-2-mediated, and in particular the BA.1-mediated, interferon response.[3,4,21] In agreement,

BA.1-mediated inhibition of H1N1 infection was abrogated in MDA5 knock-out cells (Figure 4K,L).

Taken together, our data show that BA.1-mediated suppression of H1N1 replication depends on the presence of MDA5 and is antagonized by inhibition of JAK/STAT signaling by baricitinib.

3.5 | Similar suppression of H1N1 influenza A virus replication by BA.1 and BA.5

Next, we compared the effects of BA.1 on interferon signaling and H1N1 replication to those of the Omicron subvariant BA.5 (Figure 5A).

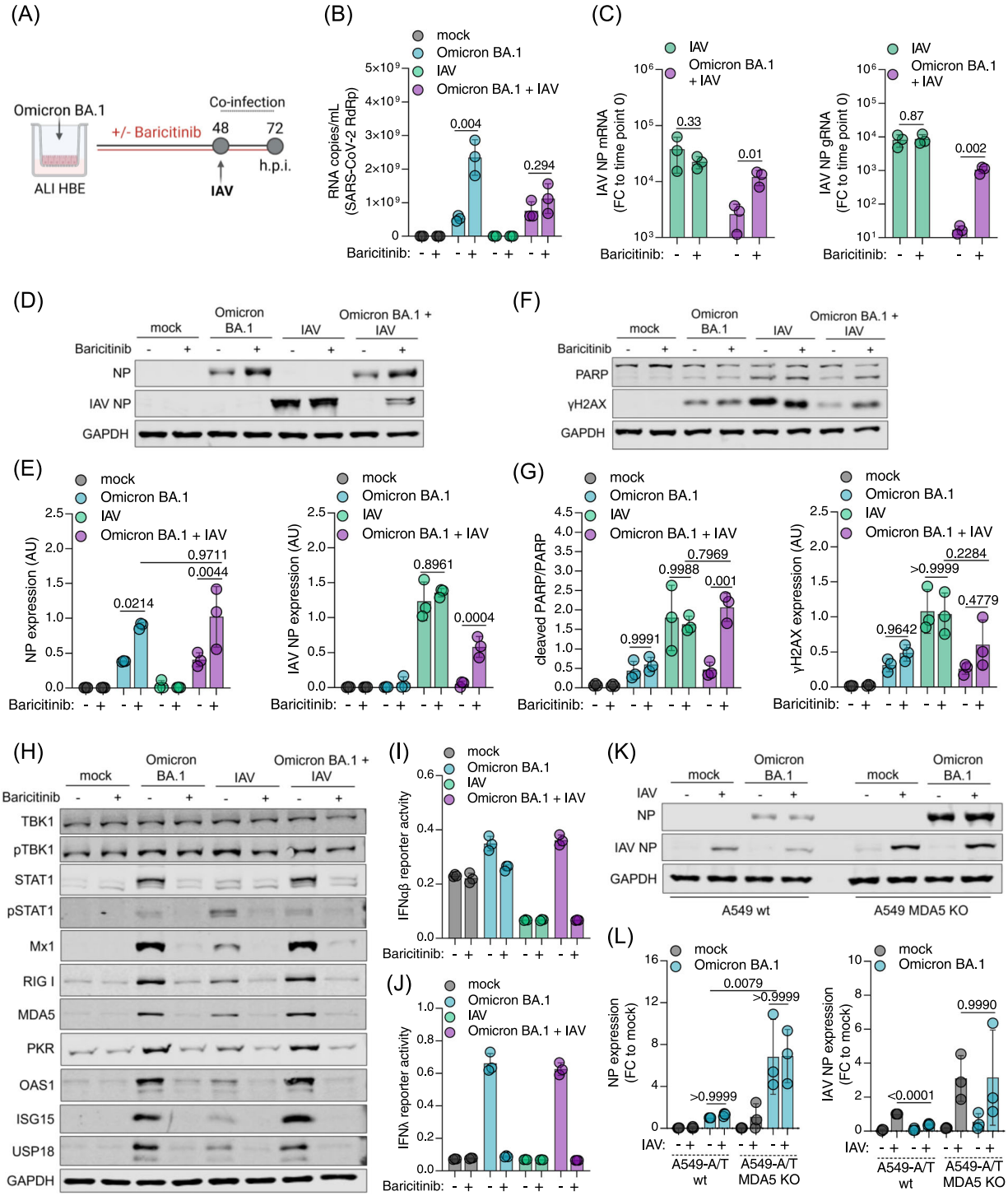

FIGURE 4 (See caption on next page)

BA.1 and BA.5 infection of ALI HBE cultures resulted in similar SARS-CoV-2 NP protein levels (Figure 5B,C) and induced similar interferon responses as indicated by the cellular levels of the interferon-stimulated gene products MX1 and ISG15 (Figure 5B) as well as interferon-α/β (Figure 5D) and -λ (Figure 5E) production in BA.1- and BA.5-infected ALI HBE cultures.

H1N1 co-infection did not significantly affect cellular SARS-CoV-2 NP levels or cellular MX1 and ISG15 levels (Figure 5F,G). However, both Omicron subvariants suppressed H1N1 replication as indicated by cellular NP levels (Figure 5F and 5H). These findings (limited impact of influenza A virus infection on SARS-CoV-2 replication, BA.1- and BA.5-mediated suppression of H1N1 replication) were confirmed by the determination of genomic SARS-CoV-2 RNA copy numbers (Figure 5I), genomic influenza A virus RNA copy numbers (Figure 5J), and H1N1 NP mRNA levels (Figure 5J). Both variants also induced similar interferon responses in the presence or absence of H1N1 as indicated by interferon-α/β (Figure 5K) and -λ (Figure 5L) production.

Taken together, BA.1 and BA.5 induce comparable interferon-mediated antiviral states in ALI HBE cultures that prevent H1N1 replication.

3.6 | BA.1-induced interferon signaling prevents H1N1 and H5N1 influenza A virus replication in primary human monocytes

Influenza A viruses can replicate in PBMCs, including CD14+ monocytes,[22] and interferon signaling in monocytes has been suggested to be a critical determinant of influenza A virus pathogenesis.[23] Highly pathogenic avian influenza A H5N1 virus has been described to replicate particularly well in monocytes and macrophages.[24–28] Hence, we investigated the impact of BA.1 and Delta on H1N1 and H5N1 virus infection in primary human monocytes (Figure 6A).

The determination of SARS-CoV-2 E RNA levels by quantitative PCR showed that BA.1 and Delta did not replicate in primary human monocytes (Figure 6B), which confirmed previous findings showing that SARS-CoV-2 causes abortive infections in monocytes.[29,30] Only BA.1 induced a pronounced interferon response as indicated by interferon α/β signaling in a HEK reporter cell line incubated with supernatants from infected monocytes (Figure 6C), MX1 mRNA levels, and ISG15 mRNA levels (Figure 6D). In contrast to the findings in ALI HBE cultures (Figures 1H, 2K, 4J, and 5L), supernatants from BA.1-infected monocytes did not induce interferon-λ activity in a HEK reporter cell line (Figure 6C).

Next, we tested the impact of BA.1 and Delta on H1N1 replication in primary human monocytes in the absence or presence of the JAK inhibitor baricitinib (Figure 6E). Neither baricitinib nor H1N1 infection affect SARS-CoV-2 E RNA levels (Figure 6F).

Similarly as in ALI HBE cultures, however, BA.1 (but not Delta) infection reduced H1N1 infection as indicated by H1N1 NP mRNA (Figure 6G) and H1N1 genomic NP RNA levels (Figure 6H), which was prevented by baricitinib (Figure 6G,H).

Highly pathogenic H5N1 avian influenza A virus also did not affect SARS-CoV-2 levels in monocytes as indicated by SARS-CoV-2 genomic E RNA levels (Figure 6I). However, the determination of H5N1 virus genomic H5 (Figure 6J) and M (Figure 6K) levels showed that abortive BA.1 but not Delta infection inhibited H5N1 replication in primary human monocytes.

Taken together, abortive BA.1 but not Delta infection induced an interferon response and reduced H1N1 and H5N1 replication in monocytes. The JAK/STAT inhibitor prevented BA.1-mediated H1N1 and H5N1 inhibition in monocytes, indicating that BA.1-mediated influenza A virus inhibition is caused by BA.1-induced interferon signaling.

3.7 | The BA.1-induced antiviral state is primarily mediated via type I interferon signaling

To confirm that BA.1 infection induces an antiviral state that is mediated by the secretion of cytokines, we tested the impact of

FIGURE 4 Inhibition of JAK/STAT signaling prevents Omicron BA.1-mediated suppression of H1N1 influenza A virus (IAV) replication in air-liquid-interface (ALI) human bronchial epithelial (HBE) cultures. (A) Experimental set-up. (B) Genomic RNA copy numbers (RNA-dependent RNA polymerase gene = RdRp) in apical washes of BA.1 (MOI 1)-infected ALI HBE cultures 72 h postinfection in the absence or presence of baricitinib 1 μM. Values represent mean ± *SD* of three biological replicates. All *p* values were determined by the Student *t*-test. (C) IAV NP mRNA (left) or genomic RNA (right) levels 24 h post-H1N1 (MOI 2) infection in the absence or presence of baricitinib 1 μM. Bars represent mean ± *SD* of three biological replicates. All *p* values were determined by the Student *t*-test. (D) Immunoblot indicating BA.1 NP and IAV NP protein levels 72 h post-BA.1 infection in the absence or presence of baricitinib 1 μM. (E) Quantification of the immunoblot results from (D) by ImageJ. Values represent mean ± *SD* of three biological replicates. All *p* values were calculated by two-way ANOVA. (F) Immunoblot indicating PARP cleavage and γH2AX protein levels 72 h post-BA.1 infection in the absence or presence of baricitinib 1 μM. (G) Quantification of the immunoblot results from (F) by ImageJ. Bars represent the quantification of the ratio between cleaved and total PARP (left) and cellular γH2AX levels (right). Values represent mean ± *SD* of three biological replicates. All *p* values were calculated by two-way ANOVA. (H) Immunoblot displaying levels of proteins involved in interferon signaling in single- and coinfected ALI HBE cultures in the absence or presence of baricitinib 1 μM. (I, J) Interferon (IFN)α/β (I) or -λ (J) activity in HEK reporter cell lines incubated with apical washes of ALI HBE cultures 72 h postinfection. (K) BA.1 NP and IAV NP protein levels in ACE2/TMPRSS2-transduced A549 (A549-A/T) cells (A549-A/T wt) or A549-A/T MDA5 knockout (KO) cells infected with BA.1 at MOI 0.01 for 24 h and followed by influenza A virus (IAV) H1N1 (MOI 2) infection for an additional 24 h. (L) Quantification of immunoblot results from (K) by ImageJ. Values represent the mean ± *SD* of three biological replicates. All *p* values were calculated by two-way ANOVA. ANOVA, analysis of variance; mRNA, messenger RNA

UV-inactivated conditioned media derived from BA.1-infected HBE ALI cultures (Figure 7A). Indeed, supernatants of BA.1-infected (but not of mock-infected) cells inhibited H1N1 infection of ARPE cells in a dose-dependent manner (Figure 7B). These effects were prevented by the addition of baricitinib to BA.1-infected cells (Figure S5), further confirming that the BA.1-induced antiviral state is mediated via interferon signaling.

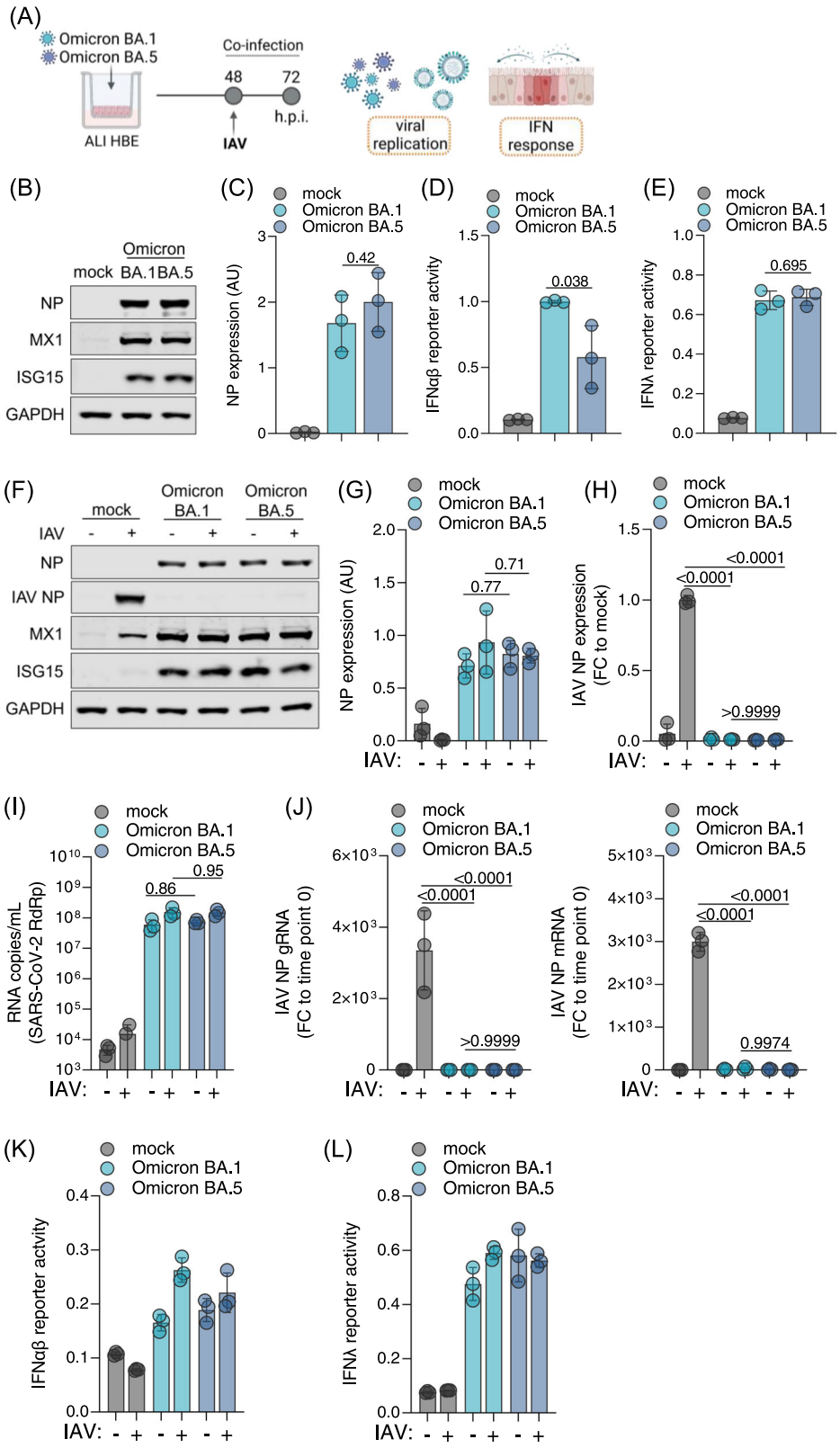

FIGURE 5 (See caption on next page)

Since baricitinib inhibits both types I and III interferon signaling, we next investigated which of the two IFN types mediates the BA.1-induced antiviral state. Only inhibition of interferon type I signaling using the vaccinia virus B18R protein (but not inhibition of interferon type III signaling using an antibody directed against the interferon-λ receptor) suppressed the antiviral state induced by conditioned media from BA.1-infected ALI HBE cultures (Figure 7C). This indicates that type I interferons are predominantly responsible for BA.1-induced inhibition of influenza A virus infection. Moreover, inhibition of interferon type I signaling completely suppressed the BA.1-mediated antiviral state in monocytes, which are known not to produce type III interferons (Figure 7D).

3.8 | Comparison of the circulation of influenza-like illnesses during the delta and BA.1 infection waves in England

An analysis comparing the spread of influenza-like illnesses (includes cases of clinically diagnosed influenza with or without a virus test confirmation) and COVID-19 in England showed that both Delta and influenza-like illnesses surged after all restrictions were removed on 19th July 2021. When BA.1 became the dominant variant, however, the number of influenza-like illnesses strongly declined and has not surged since (Figure S6). These data fit with our findings showing that BA.1 but not Delta induces an interferon response that prevents influenza A virus infection.

Similarly, three further studies reported a decrease of influenza A virus infections when the Delta variant was replaced by the Omicron variant.[31–33] Additional studies found that Omicron patients were less likely to be coinfected with influenza A viruses than Delta patients[34] and that an H3N2 outbreak in Brazil only occurred after a decline in Omicron cases.[35] Notably, such observations do not provide conclusive evidence on a potential impact of Omicron circulation on influenza A virus spread. Future research will have to investigate whether there is a causative relationship.

4 | DISCUSSION

Here, we show that only the Omicron subvariants BA.1 and BA.5 but not Delta induce the pronounced production of biologically active types I (α/β) and III (λ) interferons in infected cells (Figure S7). BA.1 infection caused an early, transient interferon-α/β peak, which is anticipated to mediate a protective antiviral response but also to avoid deleterious inflammatory processes associated with prolonged interferon type I activation.[15] Moreover, BA.1 infection caused a sustained interferon λ response known to inhibit virus replication and to prevent excessive inflammation in the respiratory tract.[15,16] Hence, these findings provide further mechanistic evidence explaining the reduced pathogenicity of Omicron relative to Delta.[17]

The BA.1- and BA.5-induced interferon responses generated an antiviral state that protected infected cells from super-infection with influenza A viruses, showing that the Omicron-induced interferon response is of functional relevance. Our analysis of the spread of influenza-like illnesses during the Delta and BA.1 infection waves (Figure S6) and a number of additional studies[31–35] suggest that Omicron may interfere with influenza A virus transmission. However, these are correlations that need to be considered with care, and a causative relationship remains to be established.

Despite consistent BA.1-mediated interferon induction across the different cell types, the relative replication kinetics of BA.1 and Delta differed between the models. BA.1 replicated less effectively than Delta in Caco-2F03 and Calu-3,[3,4] but (in agreement with other findings[13]) faster than Delta in ALI HBE cultures. This probably reflects the contribution of many factors to SARS-CoV-2 replication. The spike (S) proteins of the BA.1 and Delta isolates that we used differ in 13 amino acid positions in the S receptor binding domain (Figure S8). For example, BA.1 S is known to interact differently with its cellular receptor ACE2, to utilize ACE2 from a broader range of species as receptor, and to mediate increased virus uptake via the endosomal pathway.[36–40]

Increased Omicron uptake may also contribute to the enhanced interferon response. Mechanistically, the BA.1-induced interferon response is, in agreement with previous studies in other cell types,[3,4,21] primarily mediated by the recognition of double-

FIGURE 5 Effects of Omicron BA.1 and BA.5 on interferon signaling and H1N1 influenza A virus replication in air-liquid-interface (ALI) human bronchial epithelial (HBE) cell cultures. (A) Experimental design. (B) Cellular levels of the SARS-CoV-2 nucleoprotein (NP) and proteins involved in interferon signaling (MX1, ISG15) in BA.1- and BA.5 (MOI 1)-infected ALI HBE cultures 48 h postinfection. (C) Quantification of the NP immunoblot results from (B). Values represent mean ± *SD* from three biological replicates. All *p* values were determined by the Student *t*-test. (D, E) Interferon-α/β (D) or -λ (E) promotor activity in HEK reporter cell lines incubated with apical washes of BA.1- or BA.5-infected ALI HBE cultures 48 h postinfection. (F) SARS-CoV-2 NP (NP), influenza A virus NP (IAV NP), MX1, and ISG15 protein levels in BA.1 (MOI 1)-infected, BA.5 (MOI 1)-infected, IAV H1N1 (MOI 2)-infected, BA.1/IAV coinfected, or BA.5/IAV coinfected ALI HBE cultures. (G, H) Quantification of SARS-CoV-2 NP (G) and IAV NP (H) levels from (F) by ImageJ. (I) Genomic SARS-CoV-2 RNA (RNA-depended RNA polymerase/RdRp gene) levels in BA.1-infected, BA.5-infected, BA.1/IAV coinfected, and BA.5/IAV coinfected cells 72 h postinfection. Values represent mean ± *SD* from three biological replicates. (J) Genomic IAV NP (gRNA) copy numbers and IAV NP mRNA levels in BA.1-infected, BA.5-infected, BA.1/IAV coinfected, and BA.5/IAV coinfected cells 72 h postinfection. (K, L) Interferon-α/β (K) or -λ (L) promotor activity in HEK reporter cell lines incubated with apical washes of BA.1-infected, BA.5-infected, BA.1/IAV coinfected, and BA.5/IAV coinfected ALI HBE cultures 72 h postinfection. gRNA, guide RNA

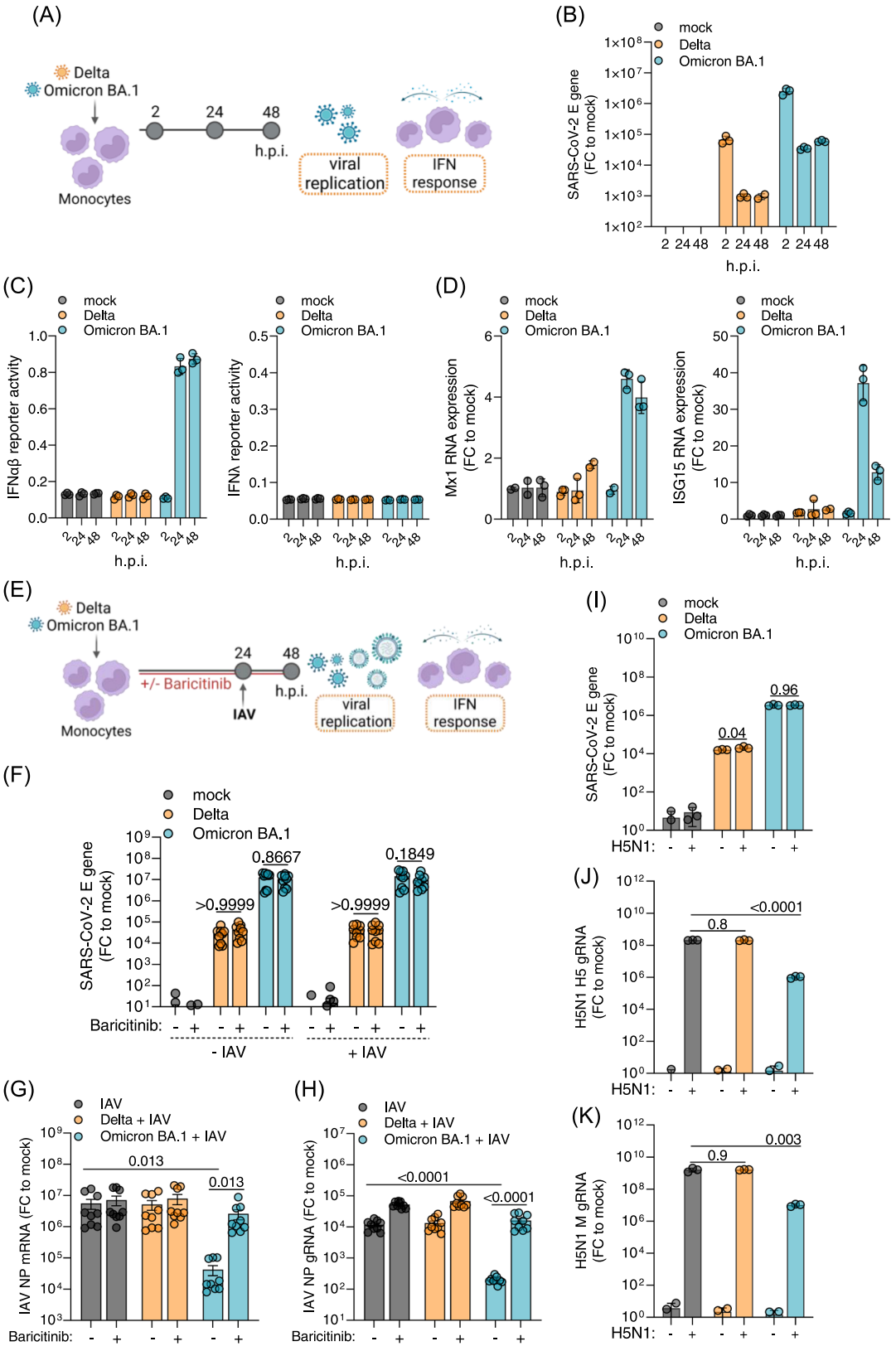

FIGURE 6 (See caption on next page)

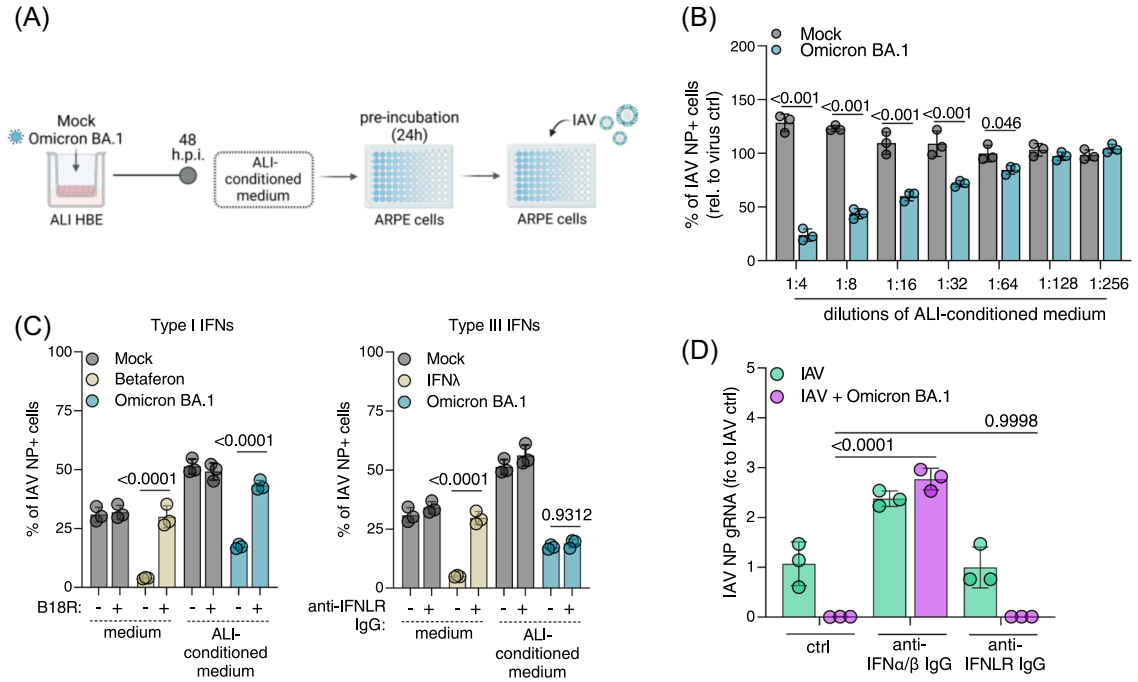

FIGURE 7 Effect of inhibition of interferon types I and III signaling on the Omicron BA.1-mediated antiviral state. (A) Experimental design underlying (B) and (C). (B) Effect of UV-inactivated conditioned media from Omicron BA.1 (MOI 1)- or mock-infected air-liquid-interface (ALI) human bronchial epithelial (HBE) cultures harvested 48 h postinfection (ALI-conditioned media) on influenza A H1N1 A/New Caledonia/20/99 virus (MOI 1) infection of ARPE cells as determined by immunofluorescence staining for influenza A virus NP 24 h postinfluenza A virus infection. (C) Effect of ARPE cell pretreatment with vaccinia virus B18R protein (inhibits type I interferon [IFN] signaling) or an anti-interferon-λ receptor 1 antibody (inhibits type III interferon signaling) on the antiviral effects of ALI-conditioned media on H1N1 infection. Betaferon (10^2 IU/mL) and IFNλ3 (1.25 μg/mL) served as positive controls. (D) Effect of interferon type I neutralizing antibodies (inhibit interferon type I signaling) or anti-interferon-λ receptor 1 antibody on H1N1 A/New Caledonia/20/99 (MOI 1) infection in BA.1 (MOI 1, 24 h)-infected primary human monocytes as determined by measuring genomic influenza A virus RNA 24 h after influenza A virus infection

stranded RNA by the pattern recognition receptor MDA5, as suggested by the lack of BA.1-induced interferon signaling in MDA5 knockout cells. Notably, virus uptake via the endosomal pathway was previously described to result in greater activation of pattern recognition receptors.[41]

BA.1 infection also induced an interferon-mediated antiviral state preventing influenza A (H1N1, H5N1) infection in monocytes despite only establishing an abortive infection, demonstrating that the antiviral state does not necessarily depend on virus replication. In agreement, UV-inactivated BA.1 was shown to trigger a detectable interferon response in lung organ cultures, although this response was weaker than that induced by the replication-competent virus.[14]

The JAK/STAT inhibitor baricitinib inhibited the BA.1-mediated antiviral response, suggesting that the Omicron-induced antiviral state is the consequence of MDA5 activation resulting in the production of interferons, which activate interferon receptors that

FIGURE 6 Impact of Omicron BA.1 and Delta on H1N1 and H5N1 influenza A virus (IAV) infection of primary human monocytes. (A) Experimental design underlying (B–D). (B) SARS-CoV-2 E gene expression levels as determined by quantitative PCR. Values represent mean ± *SD* of three biological replicates. (C) interferon-α/β (IFNα/β) (left) or IFNλ (right) activity induced by supernatants of Delta and BA.1 (MOI 1)-infected primary human monocytes in HEK-reporter cell lines. (D) Mx1 (left) and ISG15 (right) mRNA levels in Delta and BA.1 (MOI 1)-infected primary human monocytes as indicated by quantitative PCR. (E) Experimental design underlying (F–H). (F) SARS-CoV-2 E RNA levels in monocytes infected with Delta (MOI 1), BA.1 (MOI 1), Delta plus H1N1 IAV (MOI 2), or BA.1 plus H1N1 IAV (MOI 2) in the absence or presence of baricitinib 1 μM. All *p* values were determined by the Student *t*-test. (G, H) H1N1 IAV NP mRNA (G) or genomic RNA (H) levels in monocytes infected with Delta (MOI 1), BA.1 (MOI 1), Delta plus H1N1 IAV (MOI 2), or BA.1 plus H1N1 IAV (MOI 2) in the absence or presence of baricitinib 1 μM 24 h post-H1N1 IAV infection. All *p* values were calculated by two-way ANOVA. (I–K) Impact of BA.1 and Delta infection on highly pathogenic avian H5N1 IAV virus infection in monocytes. SARS-CoV-2 genomic E RNA levels (I), genomic H5N1 H5 RNA levels (J), and genomic H5N1 IAV M levels (K) in monocytes infected with Delta (MOI 1), BA.1 (MOI 1), Delta plus H5N1 strain A/Vietnam/1203/04 (MOI 1), or BA.1 plus H5N1 (MOI 1). All *p* values were calculated by two-way ANOVA. All values represent mean ± *SD* of monocyte preparations derived from three different donors (A–H) or one donor (I–K), which were each tested in three biological replicates. ANOVA, analysis of variance; mRNA, messenger RNA

then trigger JAK/STAT signaling.[42] The Omicron-induced antiviral state seems to be primarily mediated by interferon type I signaling, since only inhibition of interferon type I (but not of interferon type III) signaling suppressed the antiviral effects of conditioned media derived from BA.1-infected ALI HBE cultures and primary human monocytes.

In summary, we show that BA.1 and BA.5 (but not Delta) induce a functionally relevant pronounced interferon response that suppresses influenza A virus replication. Further research will have to show the relevance of our findings in the context of SARS-CoV-2/influenza virus co-infection. Experimental and clinical data on the severity of SARS-CoV-2/influenza A virus co-infections are inconsistent.[43–52] This may not be a surprise, given the differences in interferon signaling between different SARS-CoV-2 variants that we present here and that were described in previous studies.[3,4,14,53,54] Future studies may have to include more different virus variants and strains to establish a clearer picture.

In conclusion, our findings show that (1) BA.1 and BA.5 induce comparable interferon responses in ALI HBE cultures, (2) the Omicron-induced interferon-response is of functional relevance as it protects infected cells from influenza A virus replication, and (3) abortive BA.1 infection of monocytes is sufficient to produce a protective interferon response. Moreover, the kinetics of the Omicron-induced interferon response (early and transient type I response, sustained type III response) provide additional mechanistic evidence explaining why Omicron infections are usually associated with less severe disease than Delta infections.

AUTHOR CONTRIBUTIONS

Conceptualization: Denisa Bojkova, Martin Michaelis, Jindrich Cinatl jr.; *Investigation*: Denisa Bojkova, Marco Bechtel, T.M., Joshua D. Kandler, Lauren Hayes, Mark N. Wass Martin Michaelis, Jindrich Cinatl jr.; *Formal analysis*: all authors; *Provision of materials*: Ruth Olmer, Ulrich Martin, Danny Jonigk, Jindrich Cinatl jr; *Methods*: Denisa Bojkova, Ruth Olmer, Ulrich Martin, Danny Jonigk, Mark N. Wass, Martin Michaelis, Jindrich Cinatl jr.; *Project Administration*: Denisa Bojkova, Martin Michaelis, Jindrich Cinatl jr.; Resources: Ruth Olmer, Ulrich Martin, Danny Jonigk, Sandra Ciesek, Mark N. Wass, Jindrich Cinatl jr.; *Supervision*: Denisa Bojkova, Sandra Ciesek, Mark N. Wass, Martin Michaelis, Jindrich Cinatl jr.; *Writing—original draft*: Martin Michaelis, Jindrich Cinatl jr.; Writing—review & editing: Denisa Bojkova, Marco Bechtel, Tamara Rothenburger, Joshua D. Kandler, Lauren Hayes, Ruth Olmer, Ulrich Martin, Danny Jonigk, Sandra Ciesek, Mark N. Wass, Martin Michaelis, Jindrich Cinatl jr.

ACKNOWLEDGMENTS

We thank Lena Stegman, Kerstin Euler, and Sebastian Grothe for their technical assistance. This work was supported by the Frankfurter Stiftung für krebskranke Kinder, the Goethe-Corona-Fonds, and the BMBF (COVID-Protect, FZ: 01KI20143A).

CONFLICT OF INTEREST STATEMENT

The authors declare no conflicts of interest.

DATA AVAILABILITY STATEMENT

All data are provided in the manuscript and the related supplements.

ETHICS STATEMENT

Tissue use was approved by the ethics committee of the Hannover Medical School (MHH, Hannover, Germany, number 2701–2015) in compliance with The Code of Ethics of the World Medical Association. All patients or their next of kin gave written informed consent for the use of their lung tissue for research.

ORCID

Martin Michaelis http://orcid.org/0000-0002-5710-5888

REFERENCES

1. Bastard P, Zhang Q, Zhang SY, Jouanguy E, Casanova JL. Type I interferons and SARS-CoV-2: from cells to organisms. *Curr Opin Immunol*. 2022;74:172-182. doi:10.1016/j.coi.2022.01.003
2. Borrelli M, Corcione A, Castellano F, Fiori Nastro F, Santamaria F. Coronavirus disease 2019 in children. *Front Pediatr*. 2021;9:668484. doi:10.3389/fped.2021.668484
3. Bojkova D, Widera M, Ciesek S, Wass MN, Michaelis M, Cinatl J. Reduced interferon antagonism but similar drug sensitivity in Omicron variant compared to Delta variant of SARS-CoV-2 isolates. *Cell Res*. 2022;32(3):319-321.
4. Bojkova D, Rothenburger T, Ciesek S, Wass MN, Michaelis M, Cinatl J, Jr. SARS-CoV-2 Omicron variant virus isolates are highly sensitive to interferon treatment. *Cell Discov*. 2022;8(1):42.
5. Bojkova D, Reus P, Panosch L, et al. Identification of novel antiviral drug candidates using an optimized SARS-CoV-2 phenotypic screening platform. *iScience*. 2023;26(2):105944. doi:10.1016/j.isci.2023.105944
6. Hu B, Chan JFW, Liu H, et al. Spike mutations contributing to the altered entry preference of SARS-CoV-2 Omicron BA.1 and BA.2. *Emerg Microbes Infect*. 2022;11:2275-2287. doi:10.1080/22221751.2022.2117098
7. Shuai H, Chan JFW, Hu B, et al. Attenuated replication and pathogenicity of SARS-CoV-2 B.1.1.529 Omicron. *Nature*. 2022;603(7902):693-699. doi:10.1038/s41586-022-04442-5
8. McKellar J, Rebendenne A, Wencker M, Moncorgé O, Goujon C. Mammalian and Avian host cell influenza A restriction factors. *Viruses*. 2021;13(3):522. doi:10.3390/v13030522
9. van Wetering S, van der Linden AC, van Sterkenburg MAJA, et al. Regulation of SLPI and elafin release from bronchial epithelial cells by neutrophil defensins. *Am J Physiol Lung Cell Mol Physiol*. 2000;278(1):L51-L58. doi:10.1152/ajplung.2000.278.1.L51
10. Cinatl J, Jr., Hoever G, Morgenstern B, et al. Infection of cultured intestinal epithelial cells with severe acute respiratory syndrome coronavirus. *Cellular and Molecular Life Sciences CMLS*. 2004;61(16):2100-2112. doi:10.1007/s00018-004-4222-9
11. Bojkova D, Klann K, Koch B, et al. Proteomics of SARS-CoV-2-infected host cells reveals therapy targets. *Nature*. 2020;583(7816):469-472. doi:10.1038/s41586-020-2332-7
12. Eierhoff T, Ludwig S, Ehrhardt C. The influenza A virus matrix protein as a marker to monitor initial virus internalisation. *Biol Chem*. 2009;390(5-6):509-515. doi:10.1515/BC.2009.053
13. Hui KPY, Ho JCW, Cheung M, et al. SARS-CoV-2 Omicron variant replication in human bronchus and lung ex vivo. *Nature*. 2022;603(7902):715-720. doi:10.1038/s41586-022-04479-6
14. Alfi O, Hamdan M, Wald O, et al. SARS-CoV-2 Omicron induces enhanced mucosal interferon response compared to other variants of concern, associated with restricted replication in human lung tissues. *Viruses*. 2022;14(7):1583. doi:10.3390/v14071583

15. King C, Sprent J. Dual nature of type I interferons in SARS-CoV-2-induced inflammation. *Trends Immunol*. 2021;42(4):312-322. doi:10.1016/j.it.2021.02.003
16. Prokunina-Olsson L, Alphonse N, Dickenson RE, et al. COVID-19 and emerging viral infections: the case for interferon lambda. *J Exp Med*. 2020;217(5):e20200653. doi:10.1084/jem.20200653
17. Wang C, Liu B, Zhang S, et al. Differences in incidence and fatality of COVID-19 by SARS-CoV-2 Omicron variant versus Delta variant in relation to vaccine coverage: a world-wide review. *J Med Virol*. 2022;95. doi:10.1002/jmv.28118
18. Rani MRS, Croze E, Wei T, et al. STAT-phosphorylation–independent induction of interferon regulatory factor-9 by INTERFEROn-β. *J Interferon Cytokine Res*. 2010;30(3):163-170. doi:10.1089/jir.2009.0032
19. Li N, Parrish M, Chan TK, et al. Influenza infection induces host DNA damage and dynamic DNA damage responses during tissue regeneration. *Cell Mol Life Sci*. 2015;72(15):2973-2988. doi:10.1007/s00018-015-1879-1
20. Ampomah PB, Lim LHK. Influenza A virus-induced apoptosis and virus propagation. *Apoptosis*. 2020;25(1-2):1-11. doi:10.1007/s10495-019-01575-3
21. Yin X, Riva L, Pu Y, et al. MDA5 governs the innate immune response to SARS-CoV-2 in lung epithelial cells. *Cell Rep*. 2021;34(2):108628. doi:10.1016/j.celrep.2020.108628
22. Lersritwimanmaen P, Na-Ek P, Thanunchai M, et al. The presence of monocytes enhances the susceptibility of B cells to highly pathogenic avian influenza (HPAI) H5N1 virus possibly through the increased expression of α2,3 SA receptor. *Biochem Biophys Res Commun*. 2015;464(3):888-893. doi:10.1016/j.bbrc.2015.07.061
23. Hartshorn KL. Innate immunity and influenza A virus pathogenesis: lessons for COVID-19. *Front Cell Infect Microbiol*. 2020 Oct 22;10:563850. doi:10.3389/fcimb.2020.563850
24. Yu WCL, Chan RWY, Wang J, et al. Viral replication and innate host responses in primary human alveolar epithelial cells and alveolar macrophages infected with influenza H5N1 and H1N1 viruses. *J Virol*. 2011;85(14):6844-6855. doi:10.1128/JVI.02200-10
25. Cline TD, Beck D, Bianchini E. Influenza virus replication in macrophages: balancing protection and pathogenesis. *J Gen Virol*. 2017;98(10):2401-2412. doi:10.1099/jgv.0.000922
26. Lamichhane PP, Boonnak K, Changsom D, et al. H5N1 NS genomic segment distinctly governs the influenza virus infectivity and cytokine induction in monocytic cells. *Asian Pac J Allergy Immunol*. 2018;36(1):58-68.
27. Lamichhane PP, Puthavathana P. PR8 virus harbouring H5N1 NS gene contributed for THP-1 cell tropism. *Virusdisease*. 2018;29(4):548-552. doi:10.1007/s13337-018-0499-4
28. Westenius V, Mäkelä SM, Julkunen I, Österlund P. Highly pathogenic H5N1 influenza A virus spreads efficiently in human primary monocyte-derived macrophages and dendritic cells. *Front Immunol*. 2018;9:1664. doi:10.3389/fimmu.2018.01664
29. McLaughlin KM, Bojkova D, Kandler JD, et al. A potential role of the CD47/SIRPalpha axis in COVID-19 pathogenesis. *Curr Issues Mol Biol*. 2021;43(3):1212-1225. doi:10.3390/cimb43030086
30. Junqueira C, Crespo Â, Ranjbar S, et al. FcγR-mediated SARS-CoV-2 infection of monocytes activates inflammation. *Nature*. 2022;606(7914):576-584. doi:10.1038/s41586-022-04702-4
31. Eldesouki RE, Uhteg K, Mostafa HH. The circulation of Non-SARS-CoV-2 respiratory viruses and coinfections with SARS-CoV-2 during the surge of the Omicron variant. *J Clin Virol*. 2022;153:105215. doi:10.1016/j.jcv.2022.105215
32. Sominina A, Danilenko D, Komissarov A, et al. Resurgence of influenza circulation in the Russian Federation during the Delta and Omicron COVID-19 era. *Viruses*. 2022;14(9):1909. doi:10.3390/v14091909
33. Fratty IS, Reznik-Balter S, Nemet I, et al. Outbreak of influenza and other respiratory viruses in hospitalized patients alongside the SARS-CoV-2 pandemic. *Front Microbiol*. 2022;13:902476. doi:10.3389/fmicb.2022.902476
34. Tang CY, Boftsi M, Staudt L, et al. SARS-CoV-2 and influenza co-infection: A cross-sectional study in central Missouri during the 2021-2022 influenza season. *Virology*. 2022;576:105-110. doi:10.1016/j.virol.2022.09.009
35. Faico-Filho KS, Barbosa GR, Bellei N. Peculiar H3N2 outbreak in São Paulo during summer and emergence of the Omicron variant. *J Infect* . 2022;85(1):90-122. doi:10.1016/j.jinf.2022.04.007
36. Cameroni E, Bowen JE, Rosen LE, et al. Broadly neutralizing antibodies overcome SARS-CoV-2 Omicron antigenic shift. *Nature*. 2022;602(7898):664-670. doi:10.1038/s41586-021-04386-2
37. Hong Q, Han W, Li J, et al. Molecular basis of receptor binding and antibody neutralization of Omicron. *Nature*. 2022;604(7906):546-552. doi:10.1038/s41586-022-04581-9
38. Li L, Han P, Huang B, et al. Broader-species receptor binding and structural bases of Omicron SARS-CoV-2 to both mouse and palm-civet ACE2s. *Cell Discov*. 2022;8(1):65. doi:10.1038/s41421-022-00431-0
39. Meng B, Abdullahi A, Ferreira IATM, et al. Altered TMPRSS2 usage by SARS-CoV-2 Omicron impacts infectivity and fusogenicity. *Nature*. 2022 Mar;603(7902):706-714. doi:10.1038/s41586-022-04474-x
40. Zhang J, Cai Y, Lavine CL, et al. Structural and functional impact by SARS-CoV-2 Omicron spike mutations. *Cell Rep*. 2022 Apr 26;39(4):110729. doi:10.1016/j.celrep.2022.110729
41. Peacock TP, Goldhill DH, Zhou J, et al. The furin cleavage site in the SARS-CoV-2 spike protein is required for transmission in ferrets. *Nat Microbiol*. 2021;6(7):899-909. doi:10.1038/s41564-021-00908-w
42. Li Y, Yu P, Qu C, et al. MDA5 against enteric viruses through induction of interferon-like response partially via the JAK-STAT cascade. *Antiviral Res*. 2020;176:104743. doi:10.1016/j.antiviral.2020.104743
43. Kim EH, Nguyen TQ, Casel MAB, et al. Coinfection with SARS-CoV-2 and influenza A virus increases disease severity and impairs neutralizing antibody and CD4+ T cell responses. *J Virol*. 2022;96(6):e0187321. doi:10.1128/jvi.01873-21
44. Kim HK, Kang JA, Lyoo KS, et al. Severe acute respiratory syndrome coronavirus 2 and influenza A virus co-infection alters viral tropism and haematological composition in Syrian hamsters. *Transbound Emerg Dis*. 2022;69(5):e3297-e3304. doi:10.1111/tbed.14601
45. Oishi K, Horiuchi S, Minkoff JM, tenOever BR. The host response to influenza A virus interferes with SARS-CoV-2 replication during coinfection. *J Virol*. 2022;96(15):e0076522. doi:10.1128/jvi.00765-22
46. Cuadrado-Payán E, Montagud-Marrahi E, Torres-Elorza M, et al. SARS-CoV-2 and influenza virus co-infection. *The Lancet*. 2020;395(10236):e84. doi:10.1016/S0140-6736(20)31052-7
47. Yue H, Zhang M, Xing L, et al. The epidemiology and clinical characteristics of co-infection of SARS-CoV-2 and influenza viruses in patients during COVID-19 outbreak. *J Med Virol*. 2020;92(11):2870-2873. doi:10.1002/jmv.26163
48. Alosaimi B, Naeem A, Hamed ME, et al. Influenza co-infection associated with severity and mortality in COVID-19 patients. *Virol J*. 2021;18(1):127. doi:10.1186/s12985-021-01594-0
49. Stowe J, Tessier E, Zhao H, et al. Interactions between SARS-CoV-2 and influenza, and the impact of coinfection on disease severity: a test-negative design. *Int J Epidemiol*. 2021;50(4):1124-1133. doi:10.1093/ije/dyab081
50. Xiang X, Wang Z, Ye L, et al. Co-infection of SARS-COV-2 and influenza A virus: a case series and fast review. *Current Medical Science*. 2021;41(1):51-57. doi:10.1007/s11596-021-2317-2
51. Krumbein H, Kümmel LS, Fragkou PC, et al. Respiratory viral co-infections in patients with COVID-19 and associated outcomes: a

systematic review and meta-analysis. *Rev Med Virol*. 2022;33:e2365. doi:10.1002/rmv.2365

52. Swets MC, Russell CD, Harrison EM, et al. SARS-CoV-2 co-infection with influenza viruses, respiratory syncytial virus, or adenoviruses. *The Lancet*. 2022;399(10334):1463-1464. doi:10.1016/S0140-6736(22)00383-X
53. Guo K, Barrett BS, Morrison JH, et al. Interferon resistance of emerging SARS-CoV-2 variants. *PNAS*. 2022;119(32):e2203760119. doi:10.1073/pnas.2203760119
54. Thorne LG, Bouhaddou M, Reuschl AK, et al. Evolution of enhanced innate immune evasion by SARS-CoV-2. *Nature*. 2022;602(7897):487-495. doi:10.1038/s41586-021-04352-y

SUPPORTING INFORMATION

Additional supporting information can be found online in the Supporting Information section at the end of this article.

How to cite this article: Bojkova D, Bechtel M, Rothenburger T, et al. Omicron-induced interferon signaling prevents influenza A H1N1 and H5N1 virus infection. *J Med Virol*. 2023;95:e28686. doi:10.1002/jmv.28686